

Synthesis of Tungsten Oxide on Copper Surfaces by Electroless Deposition

Sung-Hyeon Baeck,[†] Thomas F. Jaramillo,[‡]
Galen D. Stucky,[‡] and Eric W. McFarland^{*,†}

Departments of Chemical Engineering, Chemistry
and Biochemistry, University of California,
Santa Barbara, California 93106-5080

Received March 14, 2003

Revised Manuscript Received June 2, 2003

Tungsten-based metal oxides have interesting and potentially useful electrochromic and photocatalytic properties.^{1–3} The parent of this family, tungsten oxide, has shown promise in several photoelectrochemical processes, and in these applications the formation of high surface area, mesoporous tungsten oxide would increase its applicability.^{4–7} The synthesis of mesoporous transition metal oxides has followed early work on mesoporous silica materials such as MCM-41 and SBA-15, using surfactant or polymer templates.^{8–17} Tungsten oxides, as well as oxides of several other transition metals, have been successfully synthesized electrochemically by stabilizing the metal ions in the electrolyte as a “peroxo” complex.^{1–3,18–20} Recently, we reported the electrochemical synthesis of mesoporous tungsten oxide films from an electrolyte containing a tungsten–peroxo complex as the inorganic precursor and sodium dodecyl sulfate (SDS) as the structure-directing agent; these films exhibited enhanced photocatalytic and electro-

chromic properties.²¹ There have been no reports to our knowledge of electroless deposition of polycrystalline or mesoporous metal oxide films.

Electroless deposition occurs when a species in solution is reduced onto a substrate without the aid of an external electrical power source.^{22–24} There are three fundamentally different mechanisms by which electroless deposition is conducted: autocatalytic, substrate-catalyzed, and galvanic displacement.²⁵ All three mechanisms have been used for the deposition of metals such as Au, Pt, and Pd.^{22–25} The autocatalytic process uses a complex electrolyte composition to allow the reduced metal itself to serve as a catalyst for further reductive deposition. In both the autocatalytic and the substrate-catalyzed processes, the electrolyte contains a pH buffer, a reducing agent, and oftentimes other additives. In the case of the galvanic displacement process, deposition is achieved in the absence of any external reducing agent because the reducing electrons are provided by the substrate itself. In this study, we demonstrate the electroless deposition of tungsten oxide from peroxo complex on copper substrates, and we show that it occurs by the galvanic displacement process. We also show that mesoporous tungsten oxide can be deposited by electroless plating from a solution of the tungsten–peroxo complex and surfactant templating agents.

Tungsten–peroxo electrolytes were prepared by dissolving tungsten powder in 30% hydrogen peroxide. After excess hydrogen peroxide was decomposed with platinum black, the solution was diluted to 50 mM with either a solution of water and 2-propanol (50:50) or aqueous sodium dodecyl sulfate solution (5 wt % SDS in electrolyte) for synthesis of mesoporous films. The copper substrates were used after cleaning with aqueous detergent, acetone, and 2-propanol. For each sample, a copper substrate was immersed in the electrolyte for 20 min and the resulting films were thoroughly washed with deionized water and ethanol and then dried in air. Following synthesis, scanning electron microscopy (SEM, Philips, XL-30 ESEM-FEG) was performed to show surface morphology and transmission electron microscopy (TEM, JEOL, 2000FX) was used to demonstrate mesoporosity. The oxidation states of copper substrates before and after electroless deposition were determined by X-ray photoelectron spectroscopy (XPS, Kratos, Axis Ultra). X-ray diffraction (XRD, Scintag, X2) was used to examine the sample crystal structures. For measurement of hydrogen intercalation, cyclic voltammograms were measured from –0.5 to 0 V with a Pt counter electrode vs a Ag/AgCl reference electrode in 0.5 M H₂SO₄.

The X-ray photoelectron spectra of the samples on copper substrates are shown in Figure 1a, before (A)

* To whom correspondence should be addressed. E-mail: mcfar@engineering.ucsb.edu.

[†] Department of Chemical Engineering.

[‡] Department of Chemistry and Biochemistry.

(1) Baeck, S. H.; Jaramillo, T. F.; Stucky, G. D.; McFarland, E. W. *Nano Lett.* **2002**, *2* (8), 831.

(2) Baeck, S. H.; Jaramillo, T. F.; Brondli, C.; McFarland, E. W. *J. Comb. Chem.* **2002**, *4* (6), 563.

(3) Baeck, S. H.; McFarland, E. W. *Korean J. Chem. Eng.* **2002**, *19* (4), 593.

(4) Yang, P.; Zhao, D.; Margolese, D. I.; Chmelka, B. F.; Stucky, G. D. *Nature* **1998**, *396*, 152.

(5) Cheng, W.; Baudrin, E.; Dunn, B.; J. I. Zink, J. I. *J. Mater. Chem.* **2001**, *11*, 92.

(6) Huo, Q. S.; Margolese, D. I.; Cielsla, U.; Demuth, D. G.; Feng, P. Y.; Gier, T. E.; Sieger, P.; Firouzi, A.; Chmelka, B. F.; Schuth, F.; Stucky, G. D. *Chem. Mater.* **1994**, *6*, 1176.

(7) Stein, A.; Fendorf, M.; Jarvie, T. P.; Mueller, K. T.; Benesi, A. J.; Mallouk, T. E. *Chem. Mater.* **1995**, *7*, 304.

(8) Kresge, C. T.; Leonowicz, M. E.; Roth, W. J.; Vaturi, J. C.; Beck, J. S. *Nature* **1992**, *359*, 710.

(9) Yang, P.; Deng, T.; Zhao, D.; Feng, P.; Pine, D.; Chmelka, B. F.; Whitesides, G. M.; Stucky, G. D. *Science* **1998**, *282*, 2244.

(10) Antonelli, D. M.; Ying, J. Y. *Chem. Mater.* **1996**, *8*, 874.

(11) Yang, P.; Zhao, D.; Margolese, D. I.; Chmelka, B. F.; Stucky, G. D. *Nature* **1998**, *396*, 152.

(12) Yang, P.; Zhao, D.; Margolese, D. I.; Chmelka, B. F.; Stucky, G. D. *Chem. Mater.* **1999**, *11*, 2813.

(13) Liu, P.; Lee, S.-H.; Tracy, C. E.; Yan, Y.; Turnar, J. A. *Adv. Mater.* **2002**, *14*, 27.

(14) On, D. T. *Langmuir* **1999**, *15*, 8561.

(15) Sakamoto, Y.; Kaneda, M.; Terasaki, O.; Zhao, D. Y.; Kim, J. M.; Stucky, G.; Shin, H. J.; Ryoo, R. *Nature* **2000**, *408*, 449.

(16) Ciesla, U.; Froba, M.; Stucky, G.; Schuth, F. *Chem. Mater.* **1999**, *11*, 227.

(17) Tian, B.; Liu, X.; Tu, B.; Yu, C.; Fan, J.; Wang, L.; Xie, S.; Stucky, G. D.; Zhao, D. *Nature Mater.* **2003**, *2*, 159.

(18) Pennisi, A.; Simone, F. *Sol. Energy Mater. Sol. Cells* **1992**, *28*, 233.

(19) Zhitomirsky, I. *J. Europ. Ceram. Soc.* **1999**, *19*, 2581.

(20) Zhitomirsky, I. *Mater. Lett.* **1998**, *33*, 305.

(21) Baeck, S. H.; Choi, K.-S.; Jaramillo, T. F.; Stucky, G. D.; McFarland, E. W. *Adv. Mater.* **2003**, *15* (15), 1269.

(22) Fernando, C. A. N.; Wethasinghe, S. K. *Sol. Energy Mater. Sol. Cells* **2000**, *63*, 299.

(23) Iacovangelo, C. D.; Zarnoch, K. P. *J. Electrochem. Soc.* **1991**, *138* (4), 983.

(24) Kato, M.; Sato, J.; Otani, H.; Homma, T.; Okinaka, Y.; Osaka, T.; Yoshioka, O. *J. Electrochem. Soc.* **2002**, *149* (3), C164.

(25) Poter, L. A., Jr.; Choi, H. C.; Ribbe, A. E.; Buriak, J. M. *Nano Lett.* **2002**, *2* (10), 1067.

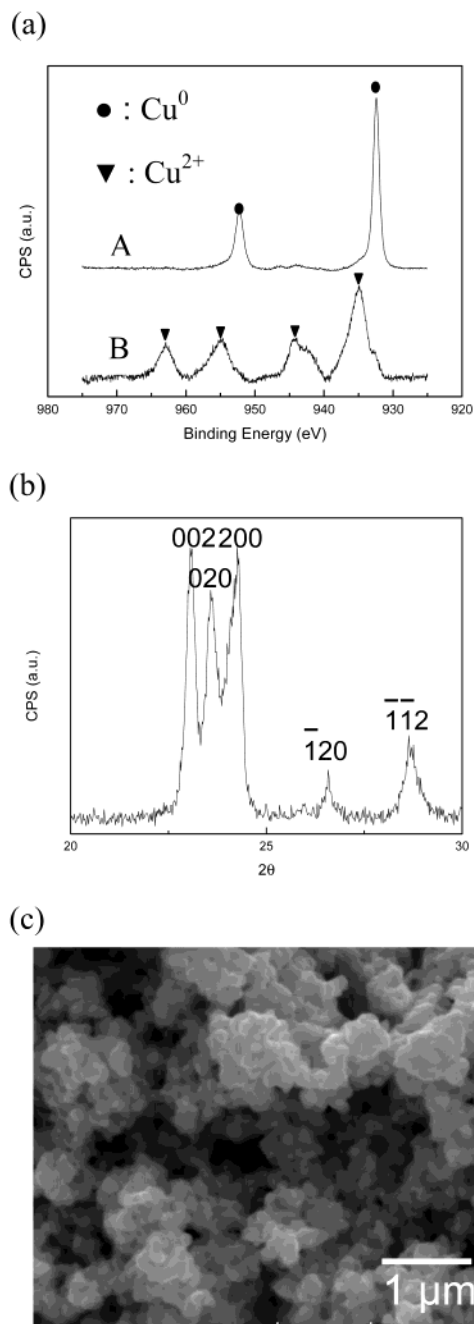


Figure 1. (a) Cu 2p XPS spectra for the copper substrate (before (A) and after (B) electroless deposition), (b) X-ray diffraction patterns of WO_3 prepared by electroless deposition after calcination at 450°C , and (c) scanning electron micrograph of WO_3 .

and after (B) electroless deposition of tungsten oxide. Before electroless plating, the oxidation state of the copper substrate is observed to be Cu^0 , with a binding energy of 952.1 and 931.3 eV. After electroless deposition, however, the four characteristic peaks of Cu^{2+} in CuO are observed at binding energies of 963.0, 954.9, 944.1, and 934.8 eV.²⁶ The large intensity of these peaks indicate that the copper substrate is oxidized primarily to CuO during electroless plating, implying the copper substrate is the source of reducing electrons and the mechanism is galvanic displacement. Shoulders are

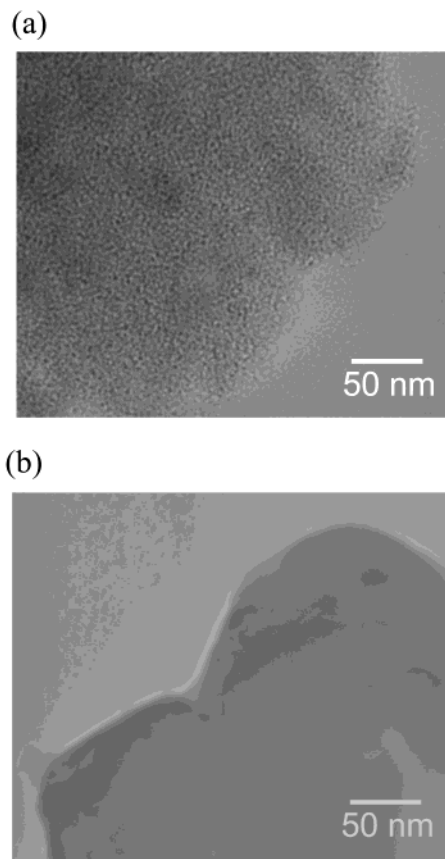


Figure 2. (a) TEM image of tungsten oxide prepared by electroless deposition with SDS and (b) TEM image of tungsten oxide prepared without SDS (control sample).

evident at 952.6 and 932.5 eV, which could be assigned to either Cu_2O or Cu metal. Conclusive evidence of the existence of Cu_2O was unattainable despite analysis of the Auger $\text{L}_{3\text{MM}}$ lines (results not shown). Nevertheless, CuO is clearly the predominant species formed at the substrate surface.

For XRD analysis, the films were removed from the substrate and calcined at 450°C for 4 h, Figure 1b. The monoclinic structure of tungsten oxide was observed.²⁷ A SEM image of the tungsten oxide film is shown in Figure 1c, revealing a rough, microporous surface. This feature is quite similar to WO_3 synthesized previously by electrodeposition.^{1–3} Thus, concerning the morphology and crystallinity of WO_3 films, the only difference between electroless deposition and electrodeposition is the source of reducing electrons—either from substrate oxidation or an external circuit.

A transmission electron micrograph (TEM) of the tungsten oxide film prepared by electroless deposition with SDS (sodium dodecyl sulfate) is shown in Figure 2a. Compared to the dense and featureless image of the WO_3 particles from the control film deposited without SDS (Figure 2b), a disordered mesoporous structure was clearly observed in Figure 2a with an average pore size of $30 \pm 4 \text{ \AA}$. The disordered mesoporous structure present in these films did not generate a small-angle X-ray diffraction peak due to the absence of long-range order. Previously, we have reported variation of the nanophases with deposition potential, which is the

(26) Espinos, J. P.; Morales, J.; Barranco, A.; Caballero, A.; Holgado, J. P.; Gonzales-Elipe, A. R. *J. Phys. Chem. B* **2002**, *106*, 6921.

(27) Ozkan, E.; Lee, S.-H.; Liu, P.; Tracy, C. E.; Tepehan, F. Z.; Pitts, J. R.; Deb., S. K. *Solid State Ionics* **2002**, *149*, 139.

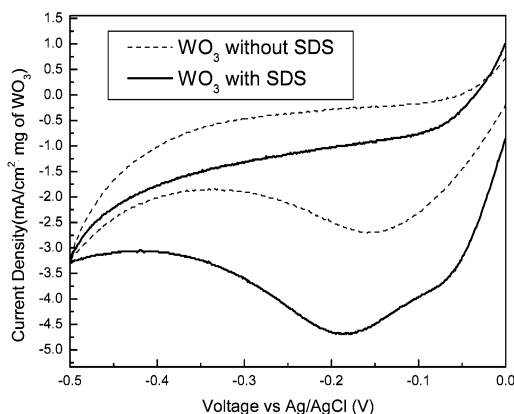


Figure 3. Cyclic voltammograms indicating hydrogen intercalation of a mesoporous tungsten oxide film (solid line) and a control film (dashed line). The current density was normalized with respect to the mass of tungsten oxide. The hydrogen intercalation capacity is measured by the area between the upper and lower lines for a given species. The figure shows a greater hydrogen intercalation capacity for the mesoporous material formed with SDS.

parameter that directly affects the surface charge densities of the electrode, and therefore, the surface assembly patterns of the inorganic-surfactant aggregates. For example, in the case of mesoporous tungsten oxide deposited at lower potentials (-0.2 V vs Ag/AgCl reference electrode), a disordered structure was observed, while at higher potentials (-0.5 V vs Ag/AgCl reference electrode) a well-ordered lamellar structure was predominant.²¹ Consistent with these findings, there is no ordered region observed in mesoporous tungsten oxides fabricated by electroless deposition.

To investigate the electrochromic properties and hydrogen capacity of the mesoporous tungsten oxide films, as-synthesized samples were measured for hydrogen intercalation. Figure 3 compares the cyclic voltammograms (measured in $0.5\text{ M H}_2\text{SO}_4$) of an electroless-deposited mesoporous tungsten oxide film synthesized with SDS (sodium dodecyl sulfate) versus a nonporous tungsten oxide film synthesized with 2-propanol. The mesoporous tungsten oxide film showed higher current density for coloration (hydrogen inter-

calation) than the nonporous tungsten oxide. This indicates that, for the same coloring current, a lower intercalation potential can be used for mesoporous tungsten oxide films. This agrees with the results we reported on nonporous and mesoporous tungsten oxide films prepared by electrodeposition.²¹ The improved efficiency for hydrogen intercalation may be attributed to the larger surface area of mesoporous tungsten oxide and to facilitated interfacial proton transfer.²¹ The double-peak shape of the cathodic current is characteristic of mesoporous tungsten oxide and has been reported previously.^{8,21} Researchers concluded that the multiple peak represented different types of hydrogen injection sites (e.g., shallow and deep trap sites), distinctive of a mesoporous structure. Because of the instability of the copper substrate during the anodic polarization of the scan, complete deintercalation was not achieved.

In summary, tungsten oxide films were successfully synthesized by electroless deposition on copper substrates from tungsten-peroxo electrolytes. The reducing electrons were provided by the copper substrate during oxidation to CuO. Mesoporous tungsten oxide was also fabricated by this method using SDS as a templating agent. Compared to nonporous tungsten oxide prepared with 2-propanol, mesoporous tungsten oxide showed greater current density for hydrogen intercalation, due to the larger surface area of mesoporous tungsten oxide and facilitated charge transport. This method can be used to fabricate molybdenum oxide, niobium oxide, zirconium oxide, and titanium oxide from metal-peroxo electrolytes.

Acknowledgment. Major funding was supported by the Hydrogen Program of the Department of Energy (DOE Grant DER-FC36-01G011092). Partial funding and facilities were provided by the National Science Foundation funded Materials Research Laboratory (Award DMR96-32716). Partial funding (G.D.S.) was also supported by the National Science Foundation (NSF Grant DMR02-33728).

CM0341641